

Accepted Manuscript

Development of ^{11}C -Labeled ω -sulfhydryl fatty acid tracer for myocardial imaging with PET

Xiangxiang Wu, Peizhi Wang, Ruixin Liu, Huahui Zeng, Fangfang Chao, Hao Liu, Caiyun Xu, Haifeng Hou, Qiong Yao

PII: S0223-5234(17)30864-4

DOI: [10.1016/j.ejmech.2017.10.062](https://doi.org/10.1016/j.ejmech.2017.10.062)

Reference: EJMECH 9854

To appear in: *European Journal of Medicinal Chemistry*

Received Date: 18 August 2017

Revised Date: 21 October 2017

Accepted Date: 21 October 2017

Please cite this article as: X. Wu, P. Wang, R. Liu, H. Zeng, F. Chao, H. Liu, C. Xu, H. Hou, Q. Yao, Development of ^{11}C -Labeled ω -sulfhydryl fatty acid tracer for myocardial imaging with PET, *European Journal of Medicinal Chemistry* (2017), doi: 10.1016/j.ejmech.2017.10.062.

This is a PDF file of an unedited manuscript that has been accepted for publication. As a service to our customers we are providing this early version of the manuscript. The manuscript will undergo copyediting, typesetting, and review of the resulting proof before it is published in its final form. Please note that during the production process errors may be discovered which could affect the content, and all legal disclaimers that apply to the journal pertain.





ACCEPTED MANUSCRIPT

Development of ^{11}C -Labeled ω -Sulfhydryl Fatty Acid Tracer for Myocardial Imaging with PET

Xiangxiang Wu^{a,||}, Peizhi Wang^{a,||}, Ruixin Liu^{a,b,||}, Huahui Zeng^{a,c,*}, Fangfang Chao^c, Hao Liu^c, Caiyun Xu^c, Haifeng Hou^c, Qiong Yao^c

^a Chinese Medicine Immunology Laboratory & Science and Technology Department, Henan University of Chinese Medicine, Zhengzhou 450046, China;

^b Department of Pharmacy, First Affiliated Hospital of Henan University of Chinese Medicine, Zhengzhou 450000, China;

^c Department of Nuclear Medicine, Second Affiliated Hospital of Zhejiang University School of Medicine, Hangzhou 310009, China.

ABSTRACT

[¹¹C]-S-methyl-16-thiopalmitic acid (**a**) was developed with excellent heart-to-background uptake ratios and higher retention in heart. Myocardial uptake and metabolism of the tracer is markedly higher CPT I dependent. When compared to [¹¹C]-S-methyl-14-thiomyristic acid (**b**), [¹¹C]-S-methyl-12-thiododecanoic acid (**c**) and [¹¹C]-palmitate, **a** showed an early high uptake and a significantly slower late clearance in heart and a prolonged myocardial elimination half-life (30 min). Analysis of heart tissue and urine samples showed that **a** was metabolized via beta-oxidation in myocardium. Small animal PET images of the accumulation of **a** in the rat myocardium were clearly superior to [¹¹C]-palmitate. These initial studies suggest that **a** could be a potentially useful clinical PET tracer to assess myocardial fatty acid metabolism.

Keywords: Fatty acid; [¹¹C]-palmitate; PET; Beta-oxidation; Myocardial imaging.

1. Introduction

Fatty acid (FA) is the primary energy substance in normal heart, which can satiate 60-80% of aerobic metabolism via the β -oxidation pathway [1]. Disturbances in FA metabolism usually reflect cardiac dysfunction, such as myocardial ischemia and heart failure [2]. Therefore, the radiolabeled FA analogs may offer an easy visualization of myocardial energy metabolism using positron emission tomography (PET) or single-photon emission computed tomography (SPECT).

Currently, a number of fatty acid-based radiopharmaceuticals have been developed to estimate myocardial metabolism by PET/SPECT and to delineate specific metabolic pathways [2]. [^{11}C]-palmitate, a classical 16-carbon FA labeled with C-11 at the C-1 position, is most commonly used for measuring myocardial FA metabolism in PET studies [3]. However, fatty acids (e.g., palmitic acid) in cardiac tissue are thoroughly degraded in a two-minute process [4]. Many groups have tried to block the oxidative degradation by insertion of an S-atom or substitution with a methyl group for a trapping effect of the tracer. 1- [^{11}C]-beta-R,S-methylheptadecanoic acid ([^{11}C]-BMHA) is the first β -methyl modified fatty acid that showed the β -oxidation process in cardiac tissue and its inhibition by the methyl group [5]. [^{11}C]-BMHA has high retention of activity in the myocardium and excellent imaging properties, because it is trapped in the cardiomyocyte owing to incomplete metabolism [4]. [^{123}I]-BMIPP, another branched-chain fatty acid, has been investigated

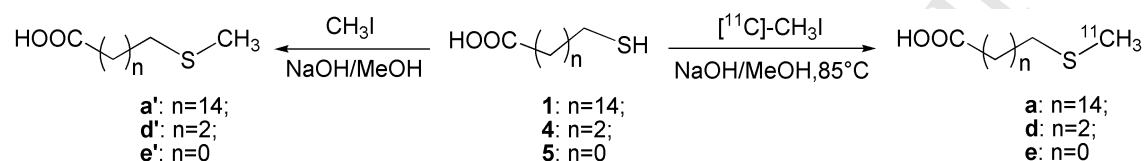
extensively and is a commercially successful cardiac SPECT agent for clinical use [6,7,8]. The thia fatty acid labeled with F-18, such as [^{18}F]-FTHA, [^{18}F]-FTO, [^{18}F]-FTP, is commonly used to estimate certain details of myocardial FA metabolism [9,10,11], which demonstrated excellent properties as myocardial PET tracers. This analog has a sulfur heteroatom substitution near the carboxyl group to block beta-oxidation of the molecule and an ^{18}F label to allow quantitative imaging with PET [12]. The technetium-99m-labeled fatty acids have been developed for many years, but none of them has a potential use in clinical practice due to its poor heart-to-background uptake ratios.

In general the modified tracers, which are labeled with various radioisotopes (e.g., F-18 or I-123), or contain other steric or functional perturbations of the FA structure (e.g., introduction of substituent group), may not be metabolized in the same way as their natural analogs do and thus may give one-sided or even misleading results. In addition, an application of FA labeled with long-lived isotope (^{18}F , ^{123}I) is not really necessary for the potential of higher image quality because of rapid catabolism of FA. Thus ^{11}C ($t_{1/2} = 20.4$ min) labeled FA analogs can be considered as a feasible alternative to radioiodinated or radio-fluorinated FA analogs. Currently, ^{11}C -labeled palmitic analog, [^{11}C]-palmitate, has been used extensively in clinical research with PET [13,14]. Since the C-11 carbon is cleaved in the initial step of β -oxidation, [^{11}C]-palmitate showed biexponential clearance from cardiac tissue, significantly complicating data analysis [4,15]. [ω - ^{11}C]-palmitate with terminal

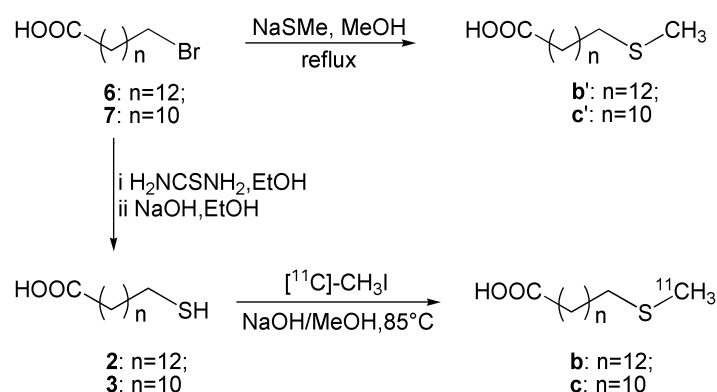
labeling with C-11 has a higher heart uptake ratio than [^{11}C]-palmitate, due to avoidance of the C-11 β -oxidation of [ω - ^{11}C]-palmitate in the initial step [16]. In spite of the progress made, the tedious synthesis process and the unstable Grignard precursor of [ω - ^{11}C]-palmitate limits its clinical application. As a result, discovering new ^{11}C -labeled fatty acid analogs that are easily synthesized and function similarly as their natural analogs in myocardium is essential for the development of the next-generation FA tracers, which still presents a major challenge in this field.

Recently, DeGrado and colleagues demonstrated that uptake of radiolabeled FA and metabolic mechanism in various tissues can be modulated by varying the structures of fatty acid. Furthermore, many research findings revealed that there was a direct relationship between the tissue distribution of the FA tracer and the calculated solvation energy level of the radiotracer and its corresponding octanol-water partition coefficients ($\log P$) [17,18]. This discovery has been shown to serve as a practical guide in design of radio-labeled fatty acid tracer [18]. We hypothesized that the introduction of the carbon-11 at the terminal of FA through sulfur atom would make it easy to produce the ^{11}C -labeled FA analog, which reflects the metabolic mechanism of its natural counterpart just as [^{11}C]-palmitate or [ω - ^{11}C]-palmitate does. Hence, ω -sulfydryl fatty acids as the precursors were coupled with [^{11}C]-methyl iodide for the efficient preparation of [^{11}C]-S-methyl-16-thiopalmitic acid ([^{11}C]-MTPA, **a**), [^{11}C]-S-methyl-14-thiomyristic acid ([^{11}C]-MTMA, **b**) and

[¹¹C]-S-methyl-12-thiododecanoic acid ([¹¹C]-MTDA, **c**). Our present study provides a simple radiosynthesis route for ¹¹C-labeled FA, and the initial results measuring myocardial uptake and metabolic mechanism of those tracers in mice. Small-animal PET imaging studies of **a** were also performed in rats and its pharmacokinetics were compared with that of [¹¹C]-palmitate.



Scheme 1. Synthesis of compounds [¹¹C]-MTPA (**a**), **d**, **e**.



Scheme 2. Synthesis of [¹¹C]-MTMA (**b**) and [¹¹C]-MTDA (**c**).

2. Results

2.1. Chemistry

The synthesis of reference compounds and radioactive tracers was performed according to Scheme 1 and 2 and characterized by ¹H-NMR, ¹³C-NMR and ESI-MS. The preparation of reference compounds (**a'**-**e'**) was based on an one-step synthetic route, i.e. methylation of ω-sulfhydryl FA with methyl iodide or substitution reaction of ω-bromo-fatty acids with NaSMe

afforded S-methyl-16-thiopalmitic acid (**a'**), S-methyl-14-thiomyristic acid (**b'**), S-methyl-12-thiododecanoic acid (**c'**), S-methyl-4-thiobutyric acid (**d'**) and S-methylthioacetic acid (**e'**) in high yield (> 63% yield). The formations of five reference compounds except for compound **e'** were characterized by the appearance of one single peak and two triplet peaks in the $^1\text{H-NMR}$ spectrum. The single peak at δ 2.10-2.13 ppm denoted three protons (CH_3S) and two triplet peaks respectively denoted two protons (CH_2CO) at δ 2.23-2.31 ppm and two protons (CH_2S) at δ 2.45-2.49 ppm. The carbon NMR spectrum verified the new methyl carbon (CH_3S) at δ 17.51-18.10 ppm and the carboxyl carbon at δ 177.08-179.90 ppm. The product formations were further confirmed by mass spectrometry. Based on these results mentioned above, compounds **a'-e'** were considered as the acceptable reference standards for evaluating the corresponding radioactive tracers.

2.2. Radiochemistry

The radiosynthesis for all radiolabeling FAs was performed using a three-step reaction sequence. First, in-target produced $[^{11}\text{C}]\text{-CO}_2$ was reduced using LiAlH_4 to $[^{11}\text{C}]\text{-CH}_3\text{OH}$ complexes; second, an iodination reaction with $[^{11}\text{C}]\text{-CH}_3\text{OH}$ complexes in the presence of hydrogen iodide aqueous afforded n.c.a $[^{11}\text{C}]\text{-CH}_3\text{I}$; finally, a methylation of the precursors (**1-5**) using $[^{11}\text{C}]\text{-methyl iodide}$ produced target compounds (**a-e**), shown in Scheme 1 & 2. After the methylation of ω -sulfhydryl fatty acids, the tracers were isolated by removal of solvent using a rotary evaporator, this also ensured the removal of $[^{11}\text{C}]\text{-methyl}$

iodide and other low molecular weight volatile [^{14}C] compounds. The evaporated residues were reconstituted with 5 mL 0.1M phosphate buffer (pH=7) and analyzed by TLC. To further identify the tracers (**a-c**), the products and their reference compounds were coinjected into analytical HPLC system using the mobile phase of acetonitrile and water containing acetic acid (0.5% v) (90/10 v/v) at a flow rate of 1 mL/min. The radio peaks of tracers are highly consistent with the UV peaks of reference compounds at the retention time of 14.1 min (**a**), 10.2 min (**b**) and 6.5 min (**c**) (Supporting Information Figure S1), indicating high radiochemical purity of tracers. HPLC analysis had produced results essentially in agreement with those using TLC analysis. The overall radiochemical yields ranged 41.4-53.1% (336-430 mCi, 12.432-15.910 GBq; decay-corrected), the radiochemical purity was almost 100%, the specific activity was estimated with about 231-301 GBq/ μmol by TLC, and the total radiosynthesis time was about 35 min, which indicated that tracers had the necessary characteristics for clinical use.

2.3. Physicochemical properties

The stability of the tracer (**a**, **b** or **c**) was determined in *ex vivo* and *in vivo* serum by using TLC. The percentage of the remaining tracer was over 97.8% in *ex vivo* serum and over 94.6% in *in vivo* serum. This stability studies demonstrated their high *in vitro/in vivo* stability to justify further investigation as myocardial imaging agents.

The solubility and biodistribution mechanism were studied by measuring octanol-water partition coefficients (log P) of the tracers. The log P values of **a**, **b** and **c** were 5.26 ± 0.03 , 4.31 ± 0.10 and 3.12 ± 0.07 , respectively. **a** showed higher log P than **b** and **c**, which indicated **a** was more hydrophobic.

Table 1. Preliminary Calculation of log P, Molecular Volume and Solvation Free Energies of the Fatty Acid Analogs. ^a

radiotracer	Molecular volume ^b	Solvation energy ^c	log P
[¹¹ C]-MTPA (a)	1079.35	-828.76	5.62(5.26) ^d
[¹¹ C]-MTMA (b)	884.54	-750.15	4.73(4.31) ^d
[¹¹ C]-MTDA (c)	797.63	-632.23	3.52(3.12) ^d
Octadecanoic acid	1082.22	-857.97	6.59
Palmitate acid	967.33	-779.36	5.72
Myristic acid	855.45	-700.75	4.90
[¹¹ C]-BMHA	1045.43	-810.38	6.41
[¹²³ I]-IPPA	1207.62	-981.84	8.27
[¹²³ I]-BMIPP	1249.55	-1021.15	8.57
[¹⁸ F]-FTHA	1022.53	-888.71	4.68
[¹⁸ F]-FTO	1077.05	-926.78	4.91
[¹⁸ F]-FTP	978.55	-826.07	4.50

^a Calculations for molecular volume, free energy of solvation and log P using Gaussian 03 implemented with b3lyp/lanl2dz.

^b The molar volume of the fatty acid analogs ($\text{cm}^3 \text{mol}^{-1}$).

^c The free energy of the fatty acid analogs in water (a.u.).

^d experimental value.

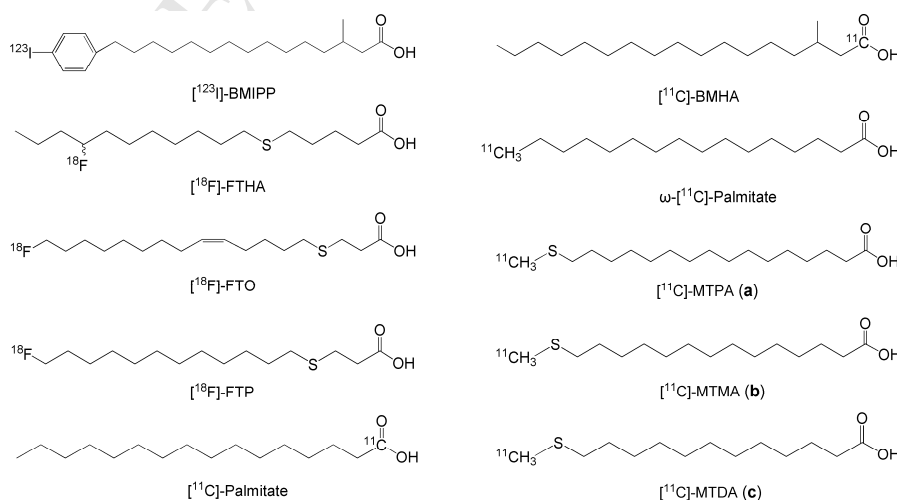


Figure 1. Radio-labeled fatty acids analogs.

The log P values and volumes of the FAs were calculated using the Gaussian 03 implemented with b3lyp/lanl2dz (Table 1 and Figure 1). The calculated values (**a**: 5.66, **b**: 4.78, **c**: 3.57) are approximate to the experimental data of the (*n*)octanol-water partition coefficients, while only log P of **a** is closely approximate to that of palmitate acid (5.72) but significantly less than that of octadecanoic acid (6.59). In comparison with the natural FAs (Octadecanoic acid, Palmitate acid, Myristic acid), the FA analogs (**a**, **b**, **c**, [¹⁸F]-FTHA, [¹⁸F]-FTO and [¹⁸F]-FTP) had been inserted by sulphur atom which was only 1.255 times volume of carbon group. The molecular volume of the radiotracers, such as **a**, [¹⁸F]-FTHA, [¹⁸F]-FTO and [¹⁸F]-FTP, is approximate to those of their natural FAs, while the rest is outside the range. The solution free energies of the FAs in water were calculated using Gaussian 03 implemented with b3lyp/lanl2dz PCM. The solvation energies of the natural FAs are between -700.75 to -857.97 a.u., only **a** (-828.76 a.u.) and **b** (-750.15 a.u.) had fallen into this range.

2.4. Biodistribution in mice

Myocardial uptake of **a** purified by HPLC or not in fasted mice was statistically unchanged respectively at 0.5, 5 and 30 min p.i., indicating higher radiochemical purity of **a** without further HPLC purification (Figure 2, Supporting Information Table S2). It was also observed that HPLC-treated **a** had slightly high uptake in heart at 0.5, 5 and 30 min postinjection (p.i.), while

there was no significant difference in the two activity uptakes in liver and kidney, demonstrating no need for further HPLC purification of **a** in the animal studies.

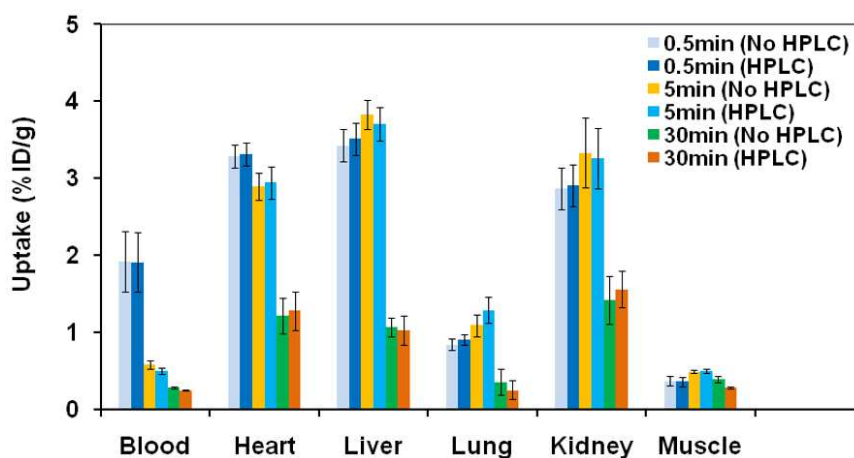


Figure 2. Comparison of heart uptake of [^{11}C]-MTPA with/without purification using HPLC at 0.5, 5 and 30 min p.i. in fasted mice.

Table 2. Biodistribution of ^{11}C -labelled Fatty Acids in Kunming Mice (%ID/g, $\bar{x}\pm\text{SD}$, n = 3)

Tissue/organ	0.5 min	5 min	10 min	30 min	60min
[^{11}C]- MTPA (a)					
Blood	1.92 \pm 0.39	0.58 \pm 0.05	0.39 \pm 0.04	0.18 \pm 0.01	0.08 \pm 0.02
Brain	0.12 \pm 0.01	0.20 \pm 0.02	0.31 \pm 0.05	0.28 \pm 0.06	0.11 \pm 0.01
Heart	3.28 \pm 0.15	2.89 \pm 0.18	2.55 \pm 0.16	1.82 \pm 0.23	0.92 \pm 0.17
Liver	3.42 \pm 0.21	3.82 \pm 0.19	2.78 \pm 0.14	1.17 \pm 0.12	1.00 \pm 0.14
Spleen	0.84 \pm 0.10	0.75 \pm 0.04	0.69 \pm 0.08	0.81 \pm 0.20	0.75 \pm 0.03
Lung	0.84 \pm 0.07	1.09 \pm 0.14	0.78 \pm 0.14	0.35 \pm 0.17	0.14 \pm 0.04
Kidney	2.87 \pm 0.27	3.33 \pm 0.45	3.32 \pm 0.21	1.42 \pm 0.31	1.20 \pm 0.27
small intestine	0.58 \pm 0.08	0.83 \pm 0.04	0.53 \pm 0.09	0.39 \pm 0.02	0.69 \pm 0.06
Muscle	0.37 \pm 0.06	0.49 \pm 0.02	0.43 \pm 0.06	0.39 \pm 0.04	0.13 \pm 0.02
Bone	0.51 \pm 0.09	0.42 \pm 0.02	0.49 \pm 0.01	0.44 \pm 0.00	0.14 \pm 0.00
Heart/Blood	1.71	4.98	6.54	10.11	11.50
Heart/Liver	0.96	0.76	0.92	1.56	0.92
Heart/Lung	3.90	2.65	3.27	5.20	6.57
[^{11}C]-MTMA (b)					
Blood	2.11 \pm 0.42	0.56 \pm 0.03	0.41 \pm 0.07	0.20 \pm 0.03	0.09 \pm 0.00
Brain	0.19 \pm 0.01	0.17 \pm 0.01	0.14 \pm 0.00	0.09 \pm 0.01	0.02 \pm 0.00
Heart	2.93 \pm 0.25	2.03 \pm 0.21	1.82 \pm 0.09	1.12 \pm 0.11	0.51 \pm 0.03
Liver	3.58 \pm 0.62	3.93 \pm 0.23	3.15 \pm 0.21	2.10 \pm 0.15	1.12 \pm 0.09
Spleen	0.93 \pm 0.08	0.80 \pm 0.07	0.73 \pm 0.08	0.66 \pm 0.07	0.54 \pm 0.07
Lung	1.45 \pm 0.65	1.33 \pm 0.08	0.74 \pm 0.11	0.40 \pm 0.05	0.15 \pm 0.01
Kidney	3.87 \pm 0.67	3.62 \pm 0.21	3.76 \pm 0.26	2.12 \pm 0.12	1.06 \pm 0.09
small intestine	0.61 \pm 0.02	0.48 \pm 0.05	0.45 \pm 0.04	0.38 \pm 0.07	0.24 \pm 0.01

Muscle	0.63 ± 0.02	0.58 ± 0.11	0.51 ± 0.06	0.42 ± 0.06	0.16 ± 0.01
Bone	0.41 ± 0.01	0.44 ± 0.06	0.45 ± 0.05	0.32 ± 0.04	0.17 ± 0.02
Heart/Blood	1.39	3.63	4.44	5.60	5.67
Heart/Liver	0.82	0.52	0.58	0.53	0.46
Heart/Lung	2.02	1.53	2.46	2.80	3.40
[¹¹C]-MTDA (c)					
Blood	1.87 ± 0.43	0.52 ± 0.02	0.44 ± 0.00	0.24 ± 0.01	0.11 ± 0.01
Brain	0.22 ± 0.05	0.21 ± 0.04	0.18 ± 0.02	0.05 ± 0.01	0.05 ± 0.00
Heart	2.37 ± 0.75	1.84 ± 0.13	1.73 ± 0.18	0.86 ± 0.22	0.25 ± 0.08
Liver	3.55 ± 0.99	3.21 ± 0.12	3.02 ± 0.13	1.38 ± 0.11	0.36 ± 0.07
Spleen	0.97 ± 0.07	0.78 ± 0.02	0.70 ± 0.03	0.34 ± 0.01	0.11 ± 0.00
Lung	1.79 ± 0.11	1.29 ± 0.34	0.87 ± 0.28	0.31 ± 0.15	0.17 ± 0.05
Kidney	3.52 ± 0.79	3.26 ± 0.32	3.39 ± 0.21	1.58 ± 0.28	0.44 ± 0.09
small intestine	0.88 ± 0.03	0.87 ± 0.04	0.78 ± 0.05	0.36 ± 0.03	0.14 ± 0.01
Muscle	0.55 ± 0.05	0.50 ± 0.01	0.46 ± 0.01	0.12 ± 0.01	0.12 ± 0.02
Bone	0.41 ± 0.04	0.50 ± 0.02	0.55 ± 0.01	0.22 ± 0.02	0.19 ± 0.03
Heart/Blood	1.27	3.54	3.94	3.58	2.27
Heart/Liver	0.67	0.57	0.57	0.62	0.69
Heart/Lung	1.32	1.43	1.99	2.77	1.47

To evaluate the pharmacokinetics of the tracers in the heart, the biodistribution experiments were performed in fasted mice. After injecting **a** into mice, high levels of radioactivity accumulated in blood, heart, liver, and kidneys at 0.5 min p.i., and the myocardial uptake washed out slowly (3.28 %ID/g at 0.5 min, 2.89 %ID/g at 5 min, 2.55 %ID/g at 10 min, 1.82 %ID/g at 30 min, and 0.92 %ID/g at 60 min p.i.) with an elimination half-life of 30 min. Furthermore, the myocardial uptakes of **a** were higher than those of **b** and **c** at all time points, indicating longer myocardial retention due to the longer FA chain of **a** (Table 2). In contrast, low uptakes of those tracers were observed in the other tissues, except for liver and kidney between 10 and 60 min. The heart-to-blood uptake ratios of **a** increased from 1.71 at 0.5 min p.i. to 11.50 at 60 min p.i., which was higher than those of **b** (from 1.39 at 0.5 min p.i. to 5.67

at 60 min p.i.) and **c** (from 1.27 at 0.5 min p.i. to 2.27 at 60 min p.i.). The heart-to-lung uptake ratios for **a** were 1.9-, and 4.5-fold higher than **b** and **c** between 30 and 60 min, respectively. Heart-to-liver uptake ratios for **a** were 2.9- and 2.5-fold higher than **b** and **c** at 30 min p.i., respectively. The results demonstrated that **a** was superior to **b** and **c** in the uptake ratios of heart-to-tissues at all time points.

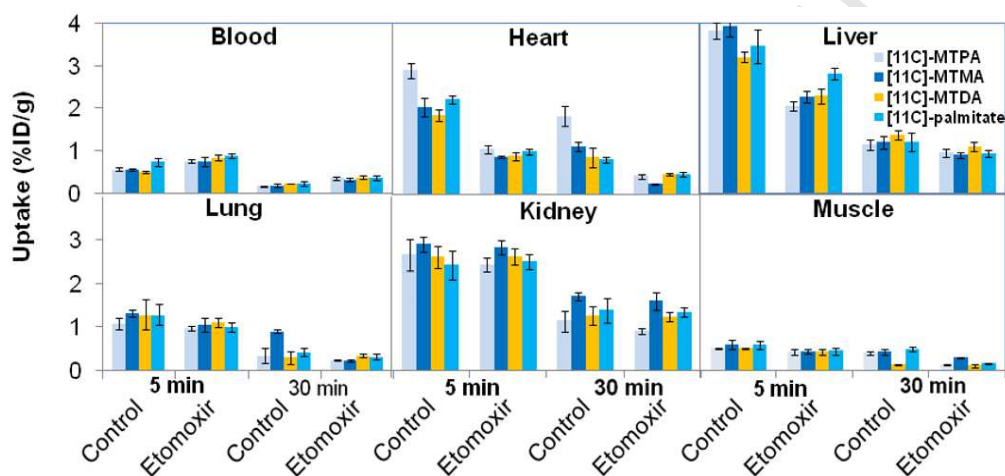


Figure 3. Biodistribution of ^{11}C -labelled fatty acids with/without etomoxir-treated at 5 and 30 min p.i. in fasted mice.

It was also observed that mice treated with etomoxir (a CPT I inhibitor) had relatively higher uptake in blood. Etomoxir-treated mice with **a**, **b**, **c** and ^{11}C -Palmitate showed 2.1-, 1.7-, 1.5- and 1.5-fold higher blood uptake at 30 min than control mice, respectively. In contrast, such enhancement with etomoxir treatment was not observed in heart, liver, lung, kidney, and muscle. For example, pretreatment of mice with etomoxir decreased the myocardial uptake of **a** by 63.7% and 76.9% at 5 and 30 min, respectively (Figure 3 and Supporting Information Table S2).

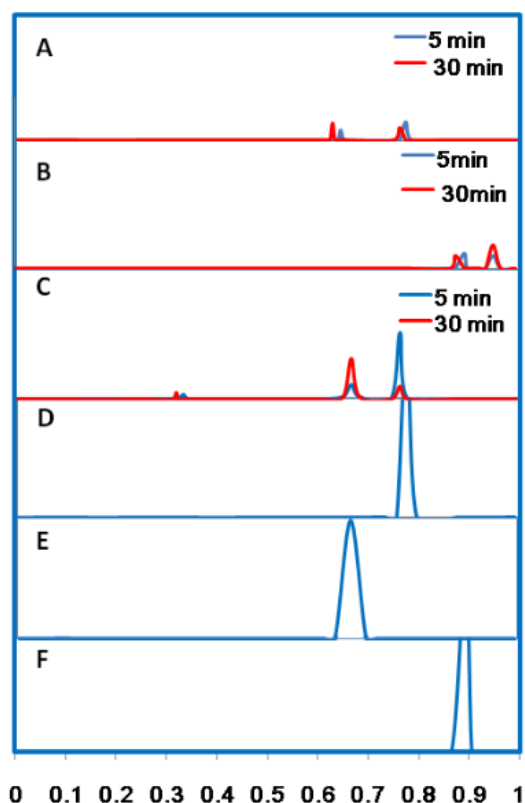


Figure 4. TLC analyses of aqueous fraction (A), organic fraction (B) and urine samples (C) obtained at 5 min and 30 min after injecting mice with [¹¹C]-MTPA (**a**), and TLC profile of **d** (D), **e** (E), **a** (F).

2.5. Metabolite analysis in mice

Radioactive metabolites of **a** were analyzed by TLC in heart tissue samples and in urine at 5 and 30 min postinjection. Analysis of aqueous fractions showed two radioactive peaks with TLC R_f values of 0.76 and 0.65, respectively, which were identified as **d** and **e** (Figure 4 A, D, E), suggesting that **a** was metabolized to **d** and **e** after six or seven cycles of β-oxidation. Analysis of the urine samples also showed the two radioactive peaks with the same R_f values except for an unidentified tiny peak (R_f = 0.32) (Figure 4C).

Analyses of the organic fractions showed the unmetabolized **a** (Figure 4 B, F) and an unidentified nonpolar compound ($R_f = 0.95$). Most of the radioactivity in control heart tissues was found in tissue pellet (57.10%, 60.51% of total at 5 and 30 min postinjection with **a**, respectively), which was significantly lower relative to **b** (68.88%, 66.61%) and **c** (65.09%, 62.24%) (Table 3). In addition, the radioactivity in tissue pellet was reduced to about half when mice were pretreated with etomoxir at 2 h before administration of **a**. The radioactivity in tissue pellet fractions of **b** and **c** were similar to **a** in the control and etomoxir-pretreated mice (Table 3).

Table 3. Distribution of Radioactivity in Heart Homogenates. (% of Total, n=3)

	Heart fraction	5min control	5min etomoxir ^a	30min control	30min etomoxir ^a
[¹¹ C]-MTPA (a)	aqueous	4.30 ± 0.19	9.85 ± 0.67	4.79 ± 0.86	6.42 ± 0.74
	organic	35.19 ± 1.23	63.21 ± 4.36	38.11 ± 1.65	70.79 ± 4.86
	pellet	60.51 ± 3.21	26.94 ± 2.42	57.10 ± 3.11	22.79 ± 1.54
[¹¹ C]-MTMA (b)	aqueous	2.78 ± 0.11	11.54 ± 1.29	3.35 ± 0.33	4.55 ± 0.53
	organic	28.34 ± 0.98	59.31 ± 4.72	30.04 ± 2.12	65.16 ± 5.21
	pellet	68.88 ± 6.21	29.15 ± 1.65	66.61 ± 2.33	30.29 ± 1.65
[¹¹ C]-MTDA (c)	aqueous	2.81 ± 0.14	12.01 ± 1.75	3.72 ± 0.65	5.12 ± 1.11
	organic	32.10 ± 2.21	57.16 ± 3.27	34.04 ± 2.75	68.50 ± 2.44
	pellet	65.09 ± 5.34	30.83 ± 2.89	62.24 ± 7.32	26.38 ± 1.42
[¹¹ C]-Palmitate	aqueous	3.56 ± 0.29	10.23 ± 0.97	4.05 ± 0.51	5.01 ± 0.39
	organic	26.45 ± 1.67	58.65 ± 3.31	34.15 ± 3.41	68.43 ± 4.75
	pellet	69.99 ± 5.63	31.12 ± 2.54	61.80 ± 6.65	26.56 ± 3.11

^a Pretreated with etomoxir (40 mg/kg ip) 2 h prior.

2.6. Small-animal PET imaging in rats

A preliminary small-animal PET imaging study was performed with **a** and [¹¹C]-palmitate in fasted rats (Figure 5). The images clearly demonstrated the high level of both tracer accumulations in the hearts, with excellent definition of

the left ventricle from the lungs, kidneys and blood pool at 30 min p.i. (Figure 5A, B). However, [^{11}C]-MTPA images displayed more excellent quality and higher activity relative to [^{11}C]-palmitate. Furthermore, there was no significant accumulation of **a** in muscle and bone. Initial dynamic images showed rapid accumulation of both tracers in the heart followed by a rapid washout within 3 min and immediate increase of radioactivity in cardiac blood pool followed by a rapid decline in approximately 5 min (Figure 5C, D). However, some differences were noted when the data were compared with the time-activity curves of [^{11}C]-palmitate. **a** was retained at a relatively high and stable level in the myocardium from 10 to 30 min after injection. In addition, the accuracy of the ROI quantitative analysis was confirmed by biodistribution experiments after the last PETscan at 30 min p.i., which showed that the PET data agreed well with the biodistribution data (Supporting Information Table S3). The results demonstrated good visualization of the heart, with excellent heart-to-background contrast at all time points, which were roughly the same as the biodistribution studies in mice, despite the different animal models used.

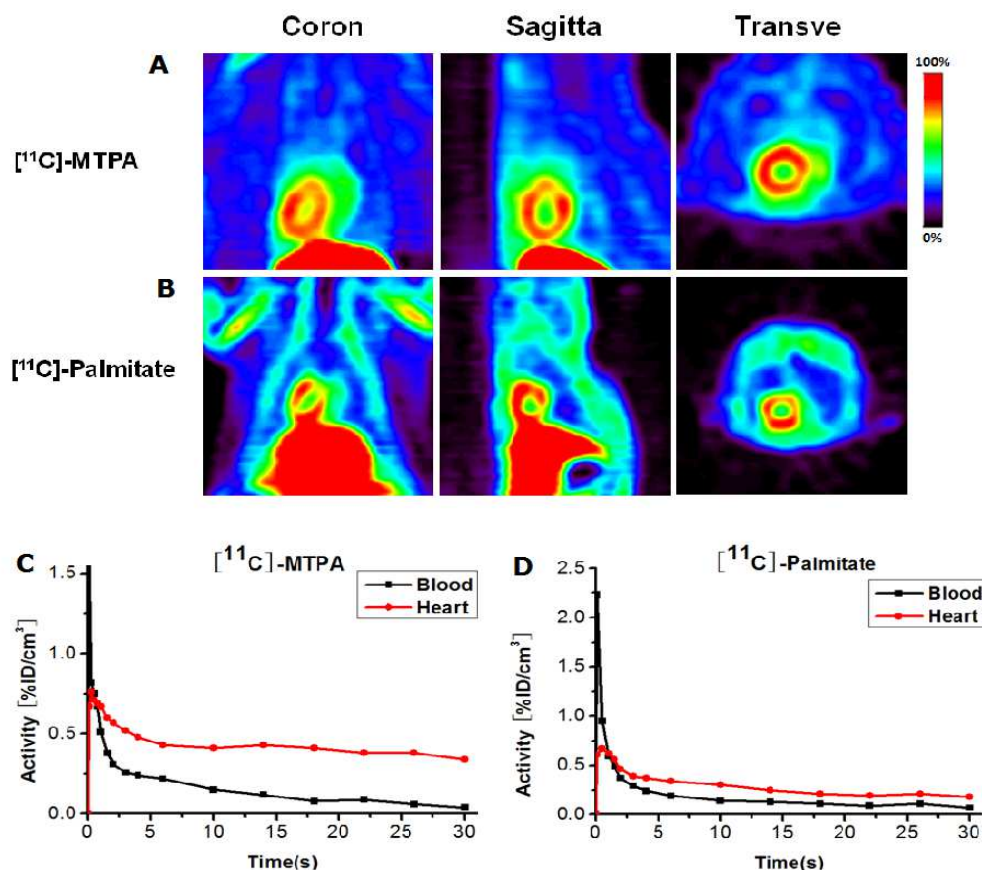


Figure 5. Representative small-animal PET images of $[^{11}\text{C}]$ -MTPA (A) and $[^{11}\text{C}]$ -palmitate (B) in fasted SD rats. Images acquired at 30-35 min p.i. are displayed on the coronal, sagittal, and transverse axis. $[^{11}\text{C}]$ -MTPA images show excellent quality and lower background than the $[^{11}\text{C}]$ -palmitate images. Time-activity curves for ROIs drawn over left ventricular wall and cardiac blood pool of rat are shown in panel C for $[^{11}\text{C}]$ -MTPA and panel D for $[^{11}\text{C}]$ -palmitate. $[^{11}\text{C}]$ -MTPA was retained at constant level in myocardium and rapidly washed out from blood.

3. Discussion

Long-chain FAs (chain length of 14-18 carbon atoms) are the major sources of energy in heart, metabolized via β -oxidation under aerobic

conditions [19]. PET imaging technique with FA-oxidation specific can improve greatly the diagnostic level of heart disease by determining myocardial viability. A variety of palmitic analogs labeled with ^{11}C , ^{18}F , or ^{123}I demonstrate excellent properties for the high uptake or retention in the myocardium. However, those tracers involve complex catabolic and anabolic processes and kinetic models to estimate the FA metabolism [4,20]. Currently, the FA radiotracers have been mostly labeled with F-18 at the terminal position, where metabolic defluorination happens in liver [21]. Conversely, the particular area of ^{11}C -labeled FA has practically been neglected since the clinical application of [^{11}C]-palmitate, although C-11 has a relatively short half life ($t_{1/2} = 20.4$ min) meaning it naturally becomes safer somewhat quickly.

We report herein the rational design and experimental validation of a mimic FA tracer (**a**) for myocardial imaging based on a FA metabolic mechanism by β -oxidation. The fatty acid chain length of 16 or 17 carbon atoms has been known to be optimal for myocardial imaging [22,23]. The sulfur atom, increasing the local polarity of **a**, substitutes for the methylene group at 17-position of octadecanoic acid, which makes the radiolabeling easier through reaction with [^{11}C]-methyl iodide. Hence, we first calculated the solvation energy, molecular volume and log P value of FA and its corresponding natural FA with density functional theory (DFT) at the b3lyp/lanl2dz. Results from our calculation revealed that the solvation energy level of **a** was between those of palmitate acid and octadecanoic acid, and the

log P value of **a** was closely approximate to that of palmitate acid but much lower than its counterpart's, while the molecular volume was approximate to its counterpart's. [¹²³I]-IPPA and [¹²³I]-BMIPP with the lowest solvation energy and the largest molecular volume and log P are different from the other tracers showed in Table 1. Thus, if the 16-thiopalmitic acid as a precursor is covalently attached to [¹¹C]-methyl group, the tracer should have the similar physical-chemical properties including log P, and the desirable biocompatibility and facile synthesis comparing to [ω -¹¹C]-palmitate and [¹¹C]-palmitate.

As a proof of concept, we developed **a** according to above calculation, which mimicked octadecanoic acid as a template molecule due to their similar structures including molecular volume. To understand the structure-bioactivity relationship of **a**, three additional radiotracers (**b**, **c**, and [¹¹C]-palmitate) were synthesized and allowed for the study of the effects of chain length (**a** vs **b**, **c**) and the ω -thia substituent (**a** vs [¹¹C]-palmitate). It was observed that **a** was superior to **b** and **c** in myocardial uptake, myocardial retention, and ratios of heart-to-tissues (blood, liver and lung) at all time points (Table 2). Here, the retention kinetics may be dependent on the length and myocardial uptake of fatty acids. In addition, **b** showed better myocardial uptake and myocardial retention than [¹¹C]-palmitate at 30 min (Figure 3 and Supporting Information Table S2), because the C-11 carbon of [¹¹C]-palmitate is cleaved in the initial step of β -oxidation, and compound **b** is just the opposite. Similarly, **a** also showed the higher myocardial uptake and better myocardial retention than

[¹¹C]-palmitate. Those results suggested that extending the chain length of the analogs (**b** or **c**) by two or four carbons to form **a** or introducing an ¹¹C-labeled methyl group at the terminal of FA through sulfur atom resulted in similar uptake and biological properties but lengthened myocardial retention. In mitochondria the transport of long-chain fatty acids are performed by the outer membrane proteins, CPT I. Pharmacologic inhibition of CPT I with etomoxir in mice was found to reduce myocardial uptake of **a** by >63.7% while reduce that of [¹¹C]-palmitate by >55.2%, demonstrating excellent sensitivity to change in myocardial FA oxidation. To further clarify the nature of the myocardial FA oxidation, a metabolite analysis experiment of **a** was performed with heart homogenates and urine samples. Radioactivity was predominantly retained in tissue pellet, and the remainder extracted was retained in the organic and the aqueous fractions. The β -oxidation metabolites, short thiafatty acid analogs such as **d** and **e**, were detected in either the aqueous fractions obtained from heart tissues or urine samples. Furthermore, the metabolite **d** as a substrate for the subsequent β -oxidation step was gradually degraded to the metabolite **e** (Figure 4A, C). In the organic fractions, a part of **a** was converted into the more nonpolar radiolabeled metabolite with time (Figure 4B). Unfortunately, this nonpolar radiolabeled metabolite in the organic fraction remains to be identified. The radioactivity in the tissue pellet, markedly higher CPT I dependent which shows high sensitivity of **a** to reflect beta oxidation rates

(Table 3), may be derived from protein-bound metabolites or other complexes similar to palmitic acid, though further research is needed to confirm that.

The alkylation reaction of sulfhydryl compound is useful for synthesizing various S-[^{11}C]-methyl- ω -sulfhydryl fatty acids [9,11]. Our synthesis procedure has greatly simplified the radiosynthesis and purification for FA tracer. The high radiochemical yield (41.4-53.1%) and radiochemical purity (approximate 100%) indicate that the synthesis procedure is an approach of choice to rapidly obtain **a** for the animal studies. Small-animal PET image of **a** in rats showed clear outline of heart during the time of study, while a defects' borders of the upper liver and the inferior heart overlapped in [^{11}C]palmitate PET image (Figure 5A, B). Due to the short biological half-life of FA in heart, the tissue time-activity curves of **a** and [^{11}C]-palmitate were consistently displayed for 0-30 min (Figure 5C, D), which provided sufficient information for measuring the kinetics of FA metabolism. **a** exhibited significant myocardial uptake and enhanced myocardial retention. However, some slight but significant differences in the time-activity curves were noted when compared with those of [^{11}C]-palmitate. For example, **a** exhibited an early activity plateau followed by a rapid early clearance in heart (at the first 3 min) and a significantly slower late clearance (at 10 min later). The time-activity curves reveal a difference in FA metabolism and washout kinetics of **a** versus [^{11}C]-palmitate due to the position of the radiolabel (S-17 position in **a** vs C-1 position in [^{11}C]-palmitate). The results

demonstrated superior myocardial imaging abilities of **a**, which could be useful for clinical PET imaging of myocardial diseases.

4. Conclusions

Three ^{11}C -labeled, thia-substituted FA analogs were rationally designed using computational chemistry and successfully synthesized with high radiochemical yield (41.4-53.1%) and radiochemical purity (approximately 100%). The tracers had suitable lipophilicity, high stability and specific activity (about 231-301 GBq/ μmol). Biodistribution and PET imaging studies of **a** were performed to validate the structure-activity relationship. The enhanced myocardial uptake and retention of **a** are primarily attributed to the longer chain length and the radiolabeling at ω -position of FA. Myocardial uptake and metabolism of the tracers appear to be markedly higher CPT I dependent. Radioactive metabolite analysis suggested that **a** was metabolized via β -oxidation in myocardium. Preliminary images of the accumulation of **a** in the rat myocardium were clearly superior to [^{11}C]-palmitate. In summary, **a** is a promising FA-oxidation tracer with the ω -thia-substituted FA analog and deserves for further preclinical evaluation.

5. Experimental section

5.1. Material and methods

Chemicals and solvents were purchased from commercial suppliers and used without additional purification. Nuclear magnetic resonance (NMR) spectra were recorded on a Bruker ARX-400 (500 MHz) spectrometer. Mass spectra (MS) were obtained with a Bruker Apex IV FTM instrument. Chromatograms of Radio-Thin Layer Chromatography (Radio-TLC) were recorded with a Bioscan System 200 (Washington, DC, USA) on 250- μ m, silica gel AL SILG/UV plates (Whatman Limited, Kent, UK). High-pressure liquid chromatography (HPLC) was performed on a Gold HPLC System equipped with a UV detector (210 nm) and a radioisotope detector. Radioactivity was measured in a dose calibrator (CRC-15R, Capintec) and tissue radioactivity in a Bioscan- γ -detector 2D-6000.

Sprague-Dawley rats (250 \pm 10 g) and Kunming mice (25 \pm 2 g) were provided by the Slac laboratory animal Co. Ltd., Shanghai. All the animal protocols were approved by the Institute's Animal Care and Use Committee and conformed to the Guide for the Care and Use of Laboratory Animals.

5.1.1. S-methyl-16-thiopalmitic acid (a'). The synthesis of the reference compound (**a'**) was conducted according to the reaction procedure illustrated in Scheme 1. The reaction flask was charged with 16-mercaptohexadecanoic acid (**1**, 1.44 g, 5 mmol), sodium hydroxide (0.40 g, 10.20 mmol) and methanol (30mL). Methyl iodide (0.32 mL, 5.1 mmol) was added to this solution and stirred at room temperature for 48 h. After its acidity and alkalinity were regulated by ethylic acid, the solvent was removed under reduced pressure.

Flash column chromatography (ethyl acetate-hexane, 10:90) gave **a'** as a pale yellow oil (0.95 g, 63.1%). ^1H NMR (500 MHz, CDCl_3) δ 1.22-1.31 (m, 22H), 1.54-1.63 (m, 4H), 2.13 (s, 3H), 2.23-2.26 (t, 2H), 2.47-2.49 (t, 2H); ^{13}C -NMR (CDCl_3 , 125 MHz) δ 18.10, 24.76, 28.55, 29.01, 29.06, 29.09, 29.66, 35.01, 36.04, 38.35, 177.08; MS (ESI): m/z 302.50 (M^+).

5.1.2. *S*-methyl-4-thiobutyric acid (**d'**). Compound **d'** was synthesized in 87.9% yield using the procedure described for **a'**. ^1H NMR (500 MHz, CDCl_3) δ 1.90-1.96 (m, 2H), 2.12 (s, 3H), 2.28-2.31 (t, 2H), 2.47-2.49 (t, 2H); ^{13}C -NMR (CDCl_3 , 125 MHz) δ 17.51, 24.36, 34.90, 35.14, 177.58; MS (ESI): m/z 134.04 (M^+).

5.1.3. *S*-methylthioacetic acid (**e'**). Compound **e'** was synthesized in 92.2% yield using the same procedure described for **a'**. ^1H NMR (500 MHz, CDCl_3) δ 2.11 (s, 3H), 3.44 (s, 2H); ^{13}C -NMR (CDCl_3 , 100 MHz) δ 17.10, 47.35, 173.12; MS (ESI): m/z 106.02 (M^+).

5.1.4. *S*-methyl-14-thiomyristic acid (**b'**). Synthesis of reference compound **b'** was performed as described in Scheme 2 [24, 25, 26]. A mixture of 14-bromomyristic acid (**4**, 1.53 g, 5 mmol) and NaSMe (0.7 g, 10 mmol) in MeOH (15 ml) was refluxed under nitrogen atmosphere for 12 h. After cooling to room temperature, the reaction mixture was poured onto ice water (80 ml), acidified with HCl (1 mol/L) to pH=1, and extracted with CHCl_3 (50 ml, 3 times). The CHCl_3 extract was dried with MgSO_4 and the solvent was removed under reduced pressure. Flash column chromatography (ethyl acetate-hexane, 10:90)

gave **b'** as a pale yellow oil (0.98 g, 71.8%). ^1H NMR (500 MHz, CDCl_3) δ 1.23-1.30 (m, 18H), 1.54-1.61 (m, 4H), 2.10 (s, 3H), 2.23-2.26 (t, 2H), 2.47-2.49 (t, 2H); ^{13}C -NMR (CDCl_3 , 125 MHz) δ 17.54, 24.81, 28.32, 28.88, 29.00, 29.35, 29.66, 30.62, 35.44, 36.29, 179.04; MS (ESI): m/z 274.6 (M^+).

5.1.5. *S*-methyl-12-thiododecanoic acid (**c'**). Compound **c'** was prepared as the synthesis of **b'** described above by coupling 12-bromododecanoic acid (**5**, 1.40 g, 5 mmol) with NaSMe (0.7 g, 10 mmol) in MeOH (15 ml), which afforded **c'** as an oil (0.96 g, 78%). ^1H NMR (500 MHz, CDCl_3) δ 1.22-1.30 (m, 14H), 1.54-1.58 (m, 4H), 2.11 (s, 3H), 2.23-2.26 (t, 2H), 2.45-2.47 (t, 2H); ^{13}C -NMR (CDCl_3 , 125 MHz) δ 17.96, 24.66, 28.45, 28.95, 29.03, 29.33, 29.92, 34.01, 34.04, 39.29, 179.90; MS (ESI): m/z 246.2 (M^+).

5.1.6. 14-mercaptomyristic acid (**2**). Synthesis of 14-mercaptomyristic acid was performed as described in the literature [27,28] (Scheme 2). A mixture of 14-bromomyristic acid (5.00 g, 16.3 mmol) and thiourea (2.10 g, 27.60 mmol) in ethanol (50 mL) was refluxed under nitrogen atmosphere for 1 day. After cooling off to room temperature, the solvent was evaporated under reduced pressure and the residue heated with NaOH (50 mL, 7.5 mol/L) for another 6 h. The mixture was carefully acidified with HCl (1 mol/L), the organic layer separated and the aqueous phase extracted as usual. Purification of the remaining raw material was accomplished by distillation under vacuum. Yield of 14-mercaptomyristic acid: 3.22 g, 76%. ^1H NMR (500 MHz, CDCl_3) δ

1.28-1.39 (m, 18H), 1.58-1.66 (m, 4H), 2.35 (t, 2H), 2.53 (m, 2H); MS (ESI): m/z 260.42 (M^+).

5.1.7. *12-mercaptododecanoic acid (3)*. 12-mercaptododecanoic acid was prepared (3.13 g, 83% yield) using a procedure similar to that used for the synthesis of compound **2** described above. ^1H NMR (500 MHz, CDCl_3) δ 1.25-1.34 (m, 14H), 1.55-1.63 (m, 4H), 2.31-2.34 (t, 2H), 2.47-2.52 (m, 2H); MS (ESI): m/z 232.40 (M^+).

5.2. Radiochemistry

Positron-emitting $[^{11}\text{C}]\text{-CO}_2$ were produced by $^{14}\text{N}(p,\alpha)^{11}\text{C}$ nuclear reactions, via proton irradiation of N_2 containing 5% O_2 using the cyclotron (HM-12; Sumitomo Heavy Industry) with target beam current set to 30 μA and irradiation time of 20 min. $[^{11}\text{C}]\text{-CO}_2$ (26-30GBq, 702-810mCi) was catalytically reduced to $[^{11}\text{C}]\text{-CH}_3\text{OH}$ complexes and iodinated in the MeI Microlab synthesis module (Sumitomo Heavy Industry) to give n.c.a $[^{11}\text{C}]\text{-CH}_3\text{I}$ which was wafted by a helium flow to a glass reaction vial containing corresponding desmethylated precursor (0.5-1 mg), methanol (0.5mL) and sodium hydroxide (0.2 mol/L, 0.05 mL) (Scheme 1, 2) [29]. $[^{11}\text{C}]\text{-Methyl iodide}$ was reacted with the precursor at 85°C for 3 min. After the reaction mixture was cooled to $\sim 20^\circ\text{C}$ and quantitatively transferred into a round flask of rotary evaporator, the solvent was removed under reduced pressure. The products were reconstituted with 5 mL 0.1M phosphate buffer (pH=7) and passed through a 0.22- μm membrane filter into a sterile multidose vial for *in vitro* and *in vivo*

experiments. The total synthesis time was about 35 min starting from [^{11}C]-carbon dioxide. The radiochemical purity analysis and identification was performed on instant thin-layer chromatography silica gel strips developed with a 30:1 ratio of methylene chloride: methanol. Subsequently the chromatographic strips were scanned on an automatic thin-layer chromatography device. The pH was determined using pH strips and sterility and pyrogen tests were analyzed according to the monographs prescribed in the Chinese Pharmacopoeia [30].

5.3. Physicochemical Properties.

The radiotracer (0.1 mCi, 100 μL) was added to 900 μL of freshly collected Kunming mice serum in a culture tube and incubated at 37 $^{\circ}\text{C}$ for 60 min. The radiotracer (0.5 mCi, 100 μL) was injected via the tail vein of Kunming mice. The blood was collected at 60 min p.i. from eyes and centrifugalized to obtain radioactivity serum. The mixture was filtered with a 0.22 μm Millipore filter and the radiochemical purity was analyzed by thin-layer chromatography. All experiments were done in triplicate.

The partition coefficients ($\log P$) of the radiotracers were measured by mixing 0.1 mL of radiotracer with *n*-octanol (5 mL) and phosphate buffer (PBS, pH 7.4, 4.9 mL) in a test tube. The test tube was vortexed for 3 min at room temperature, followed by centrifugation for 5 min at 3500 rpm. Weighted sample from the *n*-octanol and buffer layers were counted on a γ -counter. The partition coefficient was expressed as the logarithm of the ratio of the counts

per gram from *n*-octanol versus that of PBS. Sample from *n*-octanol layer was repartitioned until consistent partition of coefficient value was obtained. The measurement was done in triplicate and repeated three times.

5.4. Biodistribution

Female Kunming mice were housed for a week under a 12 h light/12 h dark cycle with free access to food and water for subsequent tissue distribution studies. Animals were fasted before experiments for 12 h. The radiotracer (0.1 ml, 100 μ Ci) was injected via the tail vein of mice ($n = 3$). The mice were killed by decapitation at 0.5, 5, 10, 30 and 60 min after injection, and the tissues and organs of interest were collected, weighed wet, and counted in a γ -counter. The radioactivity counts were corrected for the background and radioactive decay. Data are expressed as the percent injection dose per gram of tissue (%ID/g).

In another set of experiments, female Kunming mice ($n=3$) were injected intraperitoneally with a CPT-I inhibitor etomoxir (40 mg/kg) at 2 h prior to a tail-vein injection of radiotracer (**a**, **b**, **c**, [11 C]-palmitate) (0.1 ml, 100 μ Ci). The mice were killed by decapitation at 5 and 30 min p.i. The remainder of the procedure was the same as that described above

5.5. Metabolite Analysis in Mouse Hearts

After injection intraperitoneal with or without etomoxir (40 mg/kg) at 2 hours ago, mice were injected with tracers (37 MBq, 1 mCi). Samples of the heart

and the urine were collected at 5 and 30 min postinjection. The hearts were homogenized (3-5 min) in 6 mL of chloroform/methanol/40% urea/5% sulfuric acid (2:1:1:1:1) and sonicated (30 s) at 0°C. After centrifugation for 6 min at 3,000 g, aqueous, organic and residual tissue pellets were separated and counted. The urine, organic and aqueous fractions of **a** were filtered through a 0.22 µm Millipore filter, and analyzed by TLC using CH₂Cl₂-CH₃OH (15:1) as the developing solvent. Radiotracers **a**, **d**, and **e** were also analyzed by TLC using the same conditions.

5.6. Small-animal PET Imaging

A small-animal PET scanner (Concorde Microsystems, Knoxville, TN, USA) was used for *in vivo* imaging of the radiotracer (**a** and [¹¹C]-palmitate), which consisted of a 15-cm diameter ring of 96 position-sensitive γ-ray scintillation detectors, providing a 10.8-cm transaxial and a 7.8-cm axial field of view, with an image resolution of <1.8 mm. The transaxial image planes were separated by 1.21 mm. Rats were anesthetized with isoflurane (5% for induction and 2% for maintenance in oxygen at 2 L/min), placed on the scanner bed after fully anesthetized, and equipped with masks to maintain anesthesia at 2% isoflurane in oxygen at 2 L/min, and kept body temperature with infrared lamp. The dynamic acquisition for 30 min over the upper thorax and a 5-min static acquisition from 30 to 35 min were respectively performed after the intravenous administration of each tracer (18.5 MBq, 0.5 mCi). Data were collected in list mode and reconstructed by a maximum a-posteriori probability

algorithm with a pixel size of $0.4 \times 0.4 \times 1.2 \text{ mm}^3$. Round ROIs (the region of interest) of 1-2 mm diameter were drawn in the left ventricle. The signal within the ROI was expressed as percentage of injected dose per milliliter of tissue after well counter calibration of the PET scanner. To validate the accuracy of the quantitative PET data and obtain a detailed tissue distribution of **a** and [^{11}C]-palmitate, an *ex vivo* biodistribution experiment was performed. Immediately, rats were killed after the last PETscan at 30 min p.i., and tracer uptakes in the tissues/organs were recorded.

5.7. Statistical Analysis

All results are expressed as the mean \pm SD. The significance of change was analyzed using the 2-tailed Student *t* test. Statistical significance was set at $P < 0.05$. Linear regressions were performed using Pearson correlation, or exponential regression when appropriate.

Author information

Corresponding Author

* E-mail: hhzeng@hactcm.edu.cn (H. Zeng); Tel: +86-371-86566286, Fax: +86-371-65680028.

Author Contributions

¶X. Wu, P. Wang, and R. Liu contributed equally.

The manuscript was written through contributions of all authors. All authors have given approval to the final version of the manuscript.

Notes: The authors declare no competing financial interest.

Acknowledgments This project was sponsored by Natural Science Foundation of China (U1604185; 21601053; 30901190; 81773892) and the Foundation of He'nan Educational Committee (16A350007) and the Provincial Scientific Research Fund (2014KYYWF-QN07; 2014KYYWF-YQ01; 2014KYYWF-ZZCX3-04) and the Doctoral Research Fund of Henan Chinese Medicine (BSJJ2015-02).

Abbreviations used

FA, Fatty acid; PET, positron emission tomography; SPECT, single-photon emission computed tomography; $[^{123}\text{I}]$ -BMIPP, $[^{123}\text{I}]$ -15-(p-iodophenyl)-3-methylpentadecanoic acid; $[^{123}\text{I}]$ -IPPA, 4- $[^{123}\text{I}]$ -15-phenyl-pentadecanoic acid; $[^{18}\text{F}]$ -FTHA, 14-(R,S)- $[^{18}\text{F}]$ -fluoro-6-thia-heptadecanoic acid; $[^{18}\text{F}]$ -FTO, 18- $[^{18}\text{F}]$ -Fluoro-4-thia-(9Z)-octadec-9-enoic acid; $[^{18}\text{F}]$ -FTP, 18- $[^{18}\text{F}]$ -Fluoro-4-thia-palmitate; $[^{11}\text{C}]$ -BMHA, 1- $[^{11}\text{C}]$ -beta-R,S-methylheptadecanoic acid; $[^{11}\text{C}]$ -MTPA, $[^{11}\text{C}]$ -S-methyl-16-thiopalmitic acid (a); $[^{11}\text{C}]$ -MTMA, $[^{11}\text{C}]$ -S-methyl-14-thiomyristic acid (b); $[^{11}\text{C}]$ -MTDA, $[^{11}\text{C}]$ -S-methyl-12-thiododecanoic acid (c); PA, palmitate acid; NaSMe, sodium methyl mercaptide; NMR, nuclear magnetic resonance; MS, Mass spectra; TLC, Thin-Layer Chromatography; HPLC, High Performance Liquid

Chromatography; log P, octanol-water partition coefficients; R_f value, the value of the migration parameter.

References

- [1] K. Yoshinaga, N. Tamaki, Imaging myocardial metabolism, *Curr. Opin. Biotech.* 18 (2007) 52-59.
- [2] K. N Giedd, S. R. Bergmann, Fatty acid imaging of the heart, *Curr. Cardiol. Rep.* 13 (2011) 121-131.
- [3] Y. Li, T. Huang, X. Zhang, M. Zhong, N. N. Walker, J. He, S. S. Berr, S. R. Keller, B. K. Kundu, Determination of Fatty Acid Metabolism with Dynamic [^{11}C]Palmitate Positron Emission Tomography of Mouse Heart In Vivo, *Mol. Imaging* 14 (2015) 516-525.
- [4] T. M. Shoup, D. R. Elmaleh, A. A. Bonab, A. J. Fischman, Evaluation of trans-9- ^{18}F -fluoro-3,4-Methyleneheptadecanoic acid as a PET tracer for myocardial fatty acid imaging, *J. Nucl. Med.* 46 (2005) 297–304.
- [5] E. Livni, D. R. Elmaleh, S. Levy, G. L. Brownell, W. H. Strauss, Beta-methyl [$1\text{-}^{11}\text{C}$]heptadecanoic acid: a new myocardial metabolic tracer for positron emission tomography, *J. Nucl. Med.* 23 (1982)169-175.
- [6] M. Nishimura, T. Hashimoto, N. Tamaki, H. Kobayashi, T. Ono, Focal impairment in myocardial fatty acid imaging in the left anterior descending artery area, a strong predictor for cardiac death in hemodialysis patients

without obstructive coronary artery disease, *Eur. J. Nucl. Med. Mol. Imaging* 42 (2015) 1612-1621.

[7] M. Momose, K. Fukushima, C. Kondo, N. Serizawa, A. Suzuki, K. Abe, N. Hagiwara, S. Sakai, Diagnosis and Detection of Myocardial Injury in Active Cardiac Sarcoidosis-Significance of Myocardial Fatty Acid Metabolism and Myocardial Perfusion Mismatch, *Circ. J.* 79 (2015) 2669-2676.

[8] M. Pissarek, J. Meyer-Kirchrath, T. Hohlfeld, S. Vollmar, A. M. Oros-Peusquens, U. Flögel, C. Jacoby, U. Krügel, N. Schramm, Targeting murine heart and brain: visualisation conditions for multi-pinhole SPECT with ^{99m}Tc - and ^{123}I -labelled probes, *Eur. J. Nucl. Med. Mol. Imaging* 36 (2009) 1495-1509.

[9] M. K. Pandey, A. P. Belanger, S. Wang, T. R. DeGrado, Structure dependence of long-chain [^{18}F]fluorothia fatty acids as myocardial fatty acid oxidation probes, *J. Med. Chem.* 55 (2012) 10674-10684.

[10] Z. Tu, S. Li, T. L. Sharp, P. Herrero, C. S. Dence, R. J. Gropler, R. H. Mach, Synthesis and evaluation of 15-(4-(2-[^{18}F]Fluoroethoxy)phenyl)pentadecanoic acid: a potential PET tracer for studying myocardial fatty acid metabolism, *Bioconjugate Chem.* 21 (2010) 2313–2319.

[11] T. R. DeGrado, H. H. Coenen, G. Stocklin, 14-(R,S)-[^{18}F]fluoro-6-thia-heptadecanoic acid (FTHA): evaluation in mouse of a new probe of myocardial utilization of long chain fatty acids, *J. Nucl. Med.* 32 (1991) 1888-1896.

- [12] C. K. Stone, R. A. Pooley, T. R. DeGrado, B. Renstrom, R. J. Nickles, S. H. Nellis, A. J. Liedtke, J. E. Holden, Myocardial uptake of the fatty acid analog 14-fluorine-18-fluoro-6-thia-heptadecanoic acid in comparison to beta-oxidation rates by tritiated palmitate, *J. Nucl. Med.* 39 (1998) 1690-1696.
- [13] Y. Ng, S. P. Moberly, K. J. Mather, C. Brown-Proctor, G. D. Hutchins, M. A. Green, Equivalence of arterial and venous blood for [^{11}C]CO₂-metabolite analysis following intravenous administration of 1-[^{11}C]acetate and 1-[^{11}C]palmitate, *Nucl. Med. Biol.* 40 (2013) 361-365.
- [14] H. Miyabe, N. Ohte, A. Iida, H. Narita, T. Yoshida, G. Kimura, Evaluation of fatty acid beta-oxidation in patients with prior myocardial infarction in relation to myocardial blood flow, total oxidative metabolism, and left ventricular wall motion, *Circ. J.* 69 (2005) 1459-1465.
- [15] S. R. Bergmann, C. J. Weinheimer, J. Markham, P. Herrero, Quantitation of myocardial fatty acid metabolism using PET, *J. Nucl. Med.* 37 (1996) 1723–1730.
- [16] B. O. Buckman, H. F. VanBrocklin, C. S. Dence, S. R. Bergmann, M. J. Welch, J. A. Katzenellenbogen, Synthesis and tissue biodistribution of [ω - ^{11}C]palmitic acid. A novel PET imaging agent for cardiac fatty acid metabolism, *J. Med. Chem.* 37 (1994) 2481-2485.
- [17] H. Zhang, Y. Zhang, Convenient nonlinear model for predicting the tissue/blood partition coefficients of seven human tissues of neutral, acidic,

and basic structurally diverse compounds, *J. Med. Chem.* 49 (2006) 5815-5829.

[18] H. Zeng, L. Zhao, S. Hu, Y. Liu, H. Yu, N. Chen, H. Zhang, Synthesis, characterization and biodistribution of new fatty acids conjugates bearing N,N,N-donors incorporated $[\text{}^{99\text{m}}\text{Tc/Re}(\text{CO})_3]^+$, *Dalton Trans.* 42 (2013) 2894-2901.

[19] G. D. Lopaschuk, J. R. Ussher, C. D. Folmes, J. S. Jaswal, W. C. Stanley, Myocardial fatty acid metabolism in health and disease, *Physiol. Rev.* 90 (2010) 207-258.

[20] Z. Cai, N. S. Mason, C. J. Anderson, W. B. Edwards, Synthesis and preliminary evaluation of an (^{18}F) -labeled oleic acid analog for PET imaging of fatty acid uptake and metabolism, *Nucl. Med. Biol.* 43 (2016) 108-115.

[21] D. C. Moka, T. R. DeGrado, Non- β -oxidizable ω - $[^{18}\text{F}]$ fluoro long chain fatty acid analogs show cytochrome P-450-mediated defluorination: implications for the design of PET tracers of myocardial fatty acid utilization, *Int. J. Radiat. Appl. Instrum., Part B* 19 (1992) 389–397.

[22] B. C. Lee, D. H. Kim, I. Lee, Y. S. Choe, D. Y. Chi, K. H. Lee, Y. Choi, B. T. Kim, 16-Cyclopentadienyl tricarbonyl $^{99\text{m}}\text{Tc}$ 16-oxo-hexadecanoic acid: synthesis and evaluation of fatty acid metabolism in mouse myocardium, *J. Med. Chem.* 51 (2008) 3630–3634.

- [23] C. A. Otto, L. E. Brown, D. M. Wieland, W. H. Beierwaltes, Radioiodinated fatty acids for myocardial imaging: effects on chain length, *J. Nucl. Med.* 22 (1981) 613–618.
- [24] N. Iqbal, C. McEwen, S. Sardari, M. Daneshtalab, E. E. Knaus, Evaluation of Methylthio-, Methylsulfinyl-, and Methylsulfonyl- Analogs of Alkanes and Alkanoic Acids as Cardiac Inotropic and Antifungal Agents, *Arch. Pharm. Pharm. Med. Chem.* 333(2000) 293–298.
- [25] A. Pinilla, E. Mas, F. Camps, G. Fabria's, Thiafatty acids as tracers to investigate biosynthetic pathways of lepidopteran sex pheromones, *Insect Biochem. Mol. Biol.* 31 (2001) 401-405.
- [26] D. H. Kim, Y. S. Choe, J. Y. Choi, Y. Choi, K. Lee, B. Kim, 17-[4-(2-[¹⁸F]Fluoroethyl)-1H-1,2,3-triazol-1-yl]-6-thia-heptadecanoic Acid: A Potential Radiotracer for the Evaluation of Myocardial Fatty Acid Metabolism, *Bioconjugate Chem.* 20 (2009) 1139-1145.
- [27] C. M. Jung, W. Kraus, P. Leibnitz, H. Pietzsch, J. Kropp, H. Spies, Syntheses and First Crystal Structures of Rhenium Complexes Derived from ω - ω -Functionalized Fatty Acids as Model Compounds of Technetium Tracers for Myocardial Metabolism Imaging, *Eur. J. Inorg. Chem.* (2002) 1219-1225.
- [28] M. Walther, C. M. Jung, R. Bergmann, J. Pietzsch, K. Rode, K. Fahmy, P. Mirschink, S. Stehr, A. Heintz, G. Wunderlich, W. Kraus, H. J. Pietzsch, J. Kropp, A. Deussen, H. Spies, Synthesis and Biological Evaluation of a New

Type of ^{99m}Tc -Labeled Fatty Acid for Myocardial Metabolism Imaging,
Bioconjugate Chem. 18 (2007) 216-230

[29] H. Deng, X. Tang, H. Wang, G. Tang, F. Wen, X. Shi, C. Yi, K. Wu, Q. Meng, S- ^{11}C -Methyl-L-Cysteine: A New Amino Acid PET Tracer for Cancer Imaging, J. Nucl. Med. 52 (2011) 287-293.

[30] National pharmacopoeia committee. Chinese Pharmacopoeia, Chinese medical science and technology press, Beijing, Volume II (2010) 520-524.

Highlights

- ▶ Imaging fatty acid oxidation has a great potential for evaluation of myocardial diseases.
- ▶ **a** shows high myocardial uptake and retention comparable with **b**, **c** and [¹¹C]palmitate.
- ▶ **a** is a potentially useful clinical PET tracer for cardiac imaging.